Research

Landslide hazard zonation (LHZ) mapping of Doon Valley using multi-criteria analysis method based on remote sensing and GIS techniques

Ashish Mani[1,2] · Maya Kumari[1] · Ruchi Badola[2]

Abstract

The occurrence of landslides is a costly and cataclysmic natural hazard that mainly occurs in hilly areas due to factors like earthquakes, cloud burst, extreme rainfall, human pressure, etc. leading to loss of biodiversity, property, and life. Effective and comprehensive landslide risk management is crucial to address landslide susceptibility. Utilizing remote sensing and Geographic Information System (GIS) techniques, this work focuses on the landslide hazard zonation (LHZ) mapping. The study is specifically conducted in the Doon Valley. These advanced technologies help in identifying and categorizing the areas prone to landslides. The Shuttle Radar Topography Mission (SRTM) Digital Elevation Model (DEM) data at 30 m resolution and Sentinel-2B data at 10 m resolution were used to perform the remote sensing and GIS operations in ArcGIS Software. Thematic layers such as Land Use/Land Cover (LULC), Slope, Geology, Soil Type, Elevation, Drainage Density, Vegetation, and Aspect were produced utilizing remote sensing and GIS data. The weighted overlay, a multi-criteria analysis method, was applied to assign attribute values to each thematic layer based on their importance, which was then combined to calculate the landslide hazard zone. The findings of this study demonstrate that landslides are more likely to occur near and above the Main Boundary Thrust/Fault (MBT). The high to very high hazard zone covers 16.64% of the total area, making landslides occurring more frequently. Additionally, the study found that the Doon Valley rivers' upper segments are more susceptible to landslides than their lower segments. By integrating Remote Sensing and GIS techniques, it is possible to obtain extensive knowledge of regions prone to landslides. This information will be helpful for decision-makers and planners to reduce the impact of landslides in the near future.

Keywords Landslide hazard zonation (LHZ) · Weighted overlay · Disaster · Natural hazard · Doon Valley

1 Introduction

Landslides are a significant natural hazard that poses a threat to human lives, river health, and infrastructure in many regions globally [1]. The rise in human population and urbanization in hilly regions has led to a rise in the number of landslides, causing significant economic losses and loss of biodiversity globally [2].

Landslides are a significant natural hazard in India, causing extensive damage to property and biodiversity [3]. India's unique geology and climatic conditions make it particularly vulnerable to landslides, with over 12.6% of the country's landmass prone to landslides [4]. In recent years, the landslides' frequency and intensity in India have increased due to

✉ Ashish Mani, ashish.mani@s.amity.edu; Maya Kumari, mkumar10@amity.edu; Ruchi Badola, ruchi@wii.gov.in | [1]Amity School of Natural Resources and Sustainable Development, Amity University, Sector-125, Noida, Uttar Pradesh 201303, India. [2]Wildlife Institute of India, Chandrabani, Post Box #18, Dehradun, Uttarakhand 248001, India.

Discover

a lot of factors such as improper land use practices, deforestation, induced rainfall patterns, and climate change [5–7]. Landslide events in India have claimed 3971 lives over the period of 300 years in 248 fatal events. In addition to the loss of human lives, landslides in India have also caused socio-economic damage in 371 significant events [8]. Given the scale and severity of landslides in India, effective and comprehensive landslide risk management is essential. One of the essential steps in landslide risk management is the landslide hazard zonation mapping, which identifies areas susceptible to landslide occurrence. This can be accomplished by using advanced remote sensing and GIS techniques, which can provide valuable insights into the various factors contributing to landslides and help in identifying high-risk areas [9].

The application of geospatial technologies is a crucial strategy for determining landslide hazard zones. The incorporation of spatial data on geology, slope, elevation, soil, LULC, and other factors with remote sensing imagery provides an in-depth knowledge of landslide-prone areas [10–12]. This approach allows planners and decision-makers to mitigate the effects of landslides by identifying areas where preventive measures and early warning systems should be implemented.

Numerous research was done to map the landslide hazard zones utilizing remote sensing and GIS techniques [13–22]. For instance, Wang et al. in 2018 used remote sensing and GIS data to create a landslide susceptibility map of Yihuang County in China [23]. Similarly, Huang et al. in 2020 utilized remote sensing and GIS-based approaches to map landslide hazards in the Guangxi Province of China [24]. Another research by Taloor et al. [25] examined the landslide susceptibility of Doda Kishtwar ramban (DKR) region of Jammu and Kashmir based on the weighted overlay method where they found 46% of the total area over moderate to very high risk zone. Shit et al. in 2016 studied landslide risk in Maldevta, Dehradun, finding that around 33% of the area is categorized as having high to very high landslide risk using a weighted overlay model (WOM) [26].

In order to comprehend and manage landslide hazards, the current study focuses on the landslide hazard zonation mapping using remote sensing and GIS techniques. Planners and decision-makers can use a comprehensive understanding of landslide-prone areas provided by the integration of geospatial data and remote sensing imagery to mitigate the effects of landslides.

2 Study area

The Doon Valley is located in the middle of the Lesser Himalayas, and the Shiwalik mountain ranges in Uttarakhand [27]. The area is coordinated between 77° 38′ E and 78° 20′ E in longitude and 30° 01′ N to 30° 28′ N in latitude. The valley is comprised of two watersheds, Asan and Song [28]. The Asan watershed has an area of 701.15 km^2, and the Song watershed has an area of 1040.49 km^2 [29]. The outlet of the Asan watershed is in the Yamuna River, and the outlet of the Song watershed is in the Ganga River. The total area of the Doon Valley is 1741.64 km^2, with elevations that range from 303 to 2764 m. The major rivers in the Doon Valley are Bindal, Bandal, Song, Asan, Tons Rispana, and Suswa. The region receives ~ 2000 mm of average annual rainfall [30]. In general, the region experiences hot summers and chilly winters. The yearly range of temperature is between − 3 °C in the winter and 45 °C in the summer. Dehradun, Mussoorie, Vikasnagar, Doiwala, and Rishikesh are the important cities in the study area. The Study Area map is indicated below in (Fig. 1).

2.1 Methodology

3 Data and methods

In this present study, the integrated use of satellite and DEM data was used for the generation of spatial layers for the landslide hazard zonation mapping. The weighted overlay method was used to calculate a multi-criteria analysis between several raster layers. This method allows for the integration of multiple raster layers by reclassifying each layer to a common scale, assigning them relative weights based on their importance, and combining them to produce a single output raster layer. The process begins with defining the problem and identifying the relevant criteria. Next, the necessary raster layers are collected and preprocessed to ensure they have the same extent. Each raster layer is then reclassified to a standardized scale, typically from 1 to 9, where higher values represent greater risk or susceptibility. Weights are assigned to each criterion to reflect its relative importance, ensuring the total weights sum to 100%. Using the Weighted Overlay tool in ArcGIS, these reclassified layers are combined according to their assigned weights (1). The resulting output raster highlights areas of interest based on the combined influence of all criteria, facilitating informed decision-making and planning.
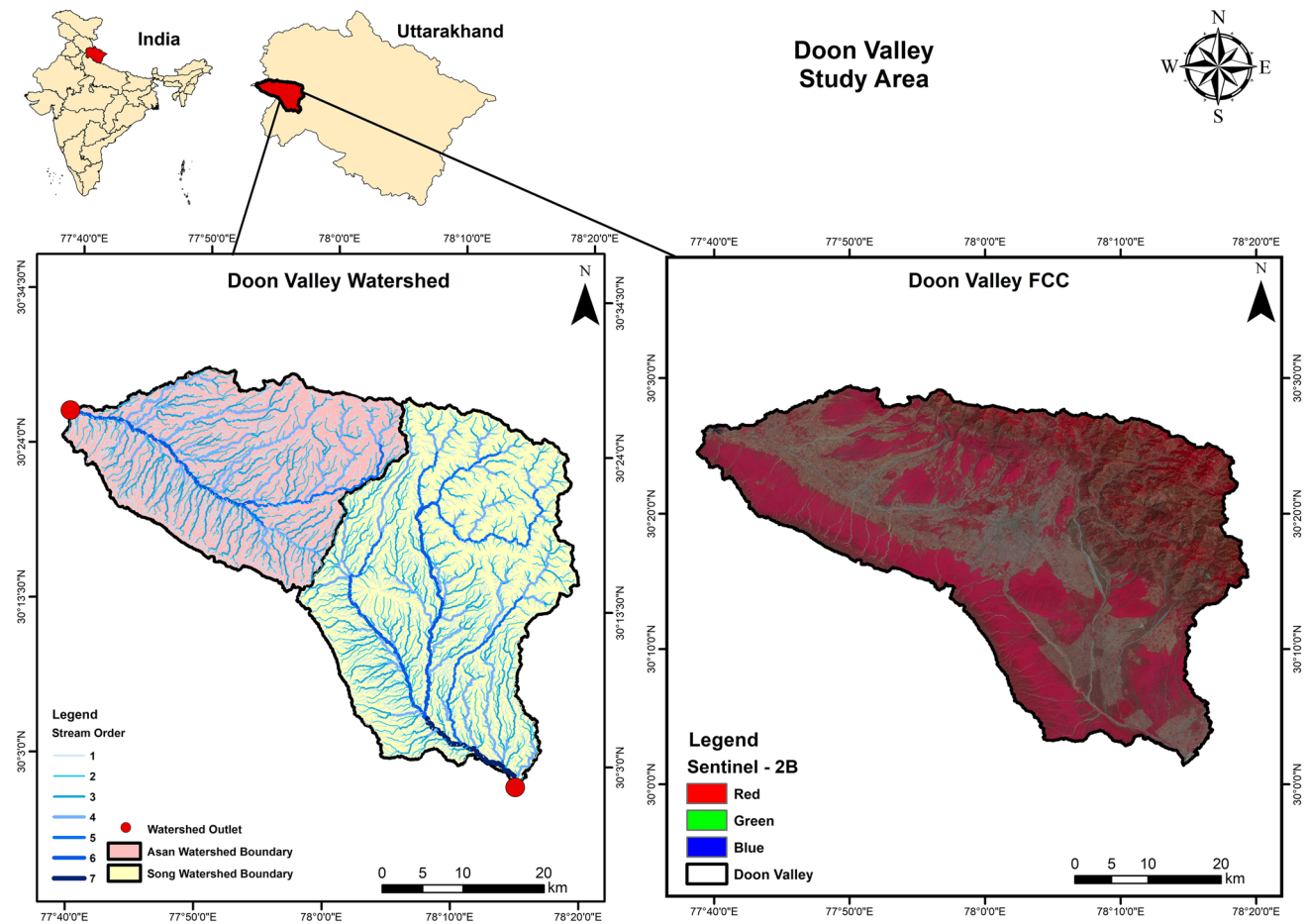
Fig. 1 The map of the study area

$$\text{Output Raster} = \sum (\text{Reclassified Raster} \times \text{Weight}) \qquad (1)$$

For the LULC classification, the supervised classification method was applied using the ERDAS Imagine software. The maximum likelihood classifier was used to identify each training samples. Based on the training samples, the LULC classes was defined. The ArcGIS software was used to create maps of the Doon Valley's aspect, slope, elevation, geology, drainage density, vegetation, LULC, soil, and landslide hazard zone. The source of data and flow chart of the methodology explained in Table 1 and Fig. 2.

### 3.1 Flowchart of the methodology

See Fig. 2.

4 Results and discussion

4.1 Slope

The area's steepness is indicated by the slope [31]. According to Fig. 3, the Doon Valley slope is categorized into five classes: (0° to ≤ 5°) is very gentle, having 50.01% of the total area, (> 5° to ≤ 15°) is gentle, having 21.21% of the

Table 1 Data source and data type

Sr. No	Data source and type	Data layers
1	Sentinel-2B satellite imagery (19/04/2022) downloaded from ESA-Copernicus data hub	LULC and vegetation
2	SRTM DEM at 30 m resolution (23/09/2014) downloaded from USGS Earth Explorer	Slope, elevation, aspect, drainage density and watershed
3	ICAR-NBSS&LUP, Bhoomi Geoportal, India Soil at 1:1 M scale	Soil
4	Western Kumaon Himalayas map by Rupke & Sharma in 1974 is Georeferenced through ArcGIS software	Geology
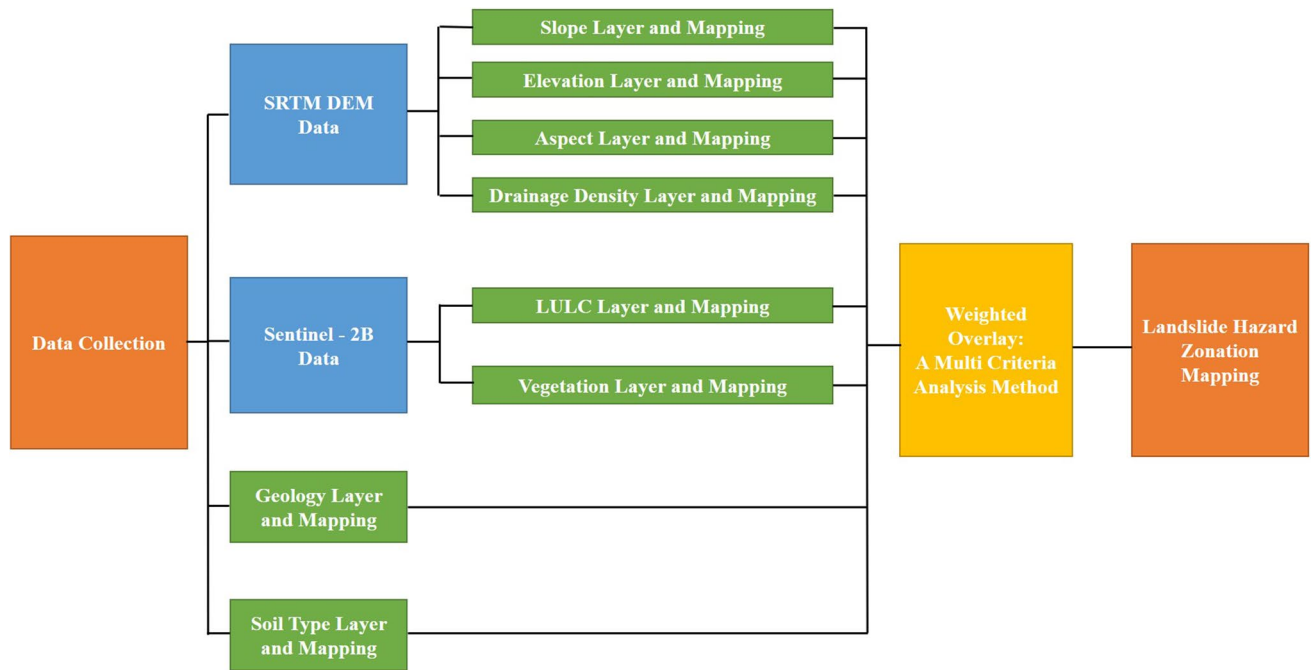
Fig. 2 Flowchart

total area, (> 15° to ≤ 30°) is Moderate having 16.77% of the total area, (> 30° to ≤ 45°) is steep having 10.84% of total area and (> 45° to 75°) is very steep having 1.17% of total area. The table and map make it clear that half of the area is having very gentle slope (Table 2). With little runoff and a gradual slope, the valley is favorable for groundwater penetration. Based on how frequently certain slope angles occur, slope categories are defined by slope maps. The geomorphological history of the landscape determines how the slope categories are distributed [32].

4.2 Elevation

According to Fig. 4 & Table 3, there are five different elevation classifications in the Doon Valley: (≤ 600 m) is very low, having 38.96% of the total area, (> 600 m to ≤ 900 m) is low, having 35.47% of the total area, (> 900 m to ≤ 1200 m) is moderate having 7.55% of the total area, > 1200 m to ≤ 1600 m) is high having 8.4% of the total area and > 1600 m to 2764 m) is very high having 9.62% of the total area. Most of the area has an elevation value that is low to very low, indicating that elevation and drainage density are related indirectly, whereas elevation and slope are related directly [33].
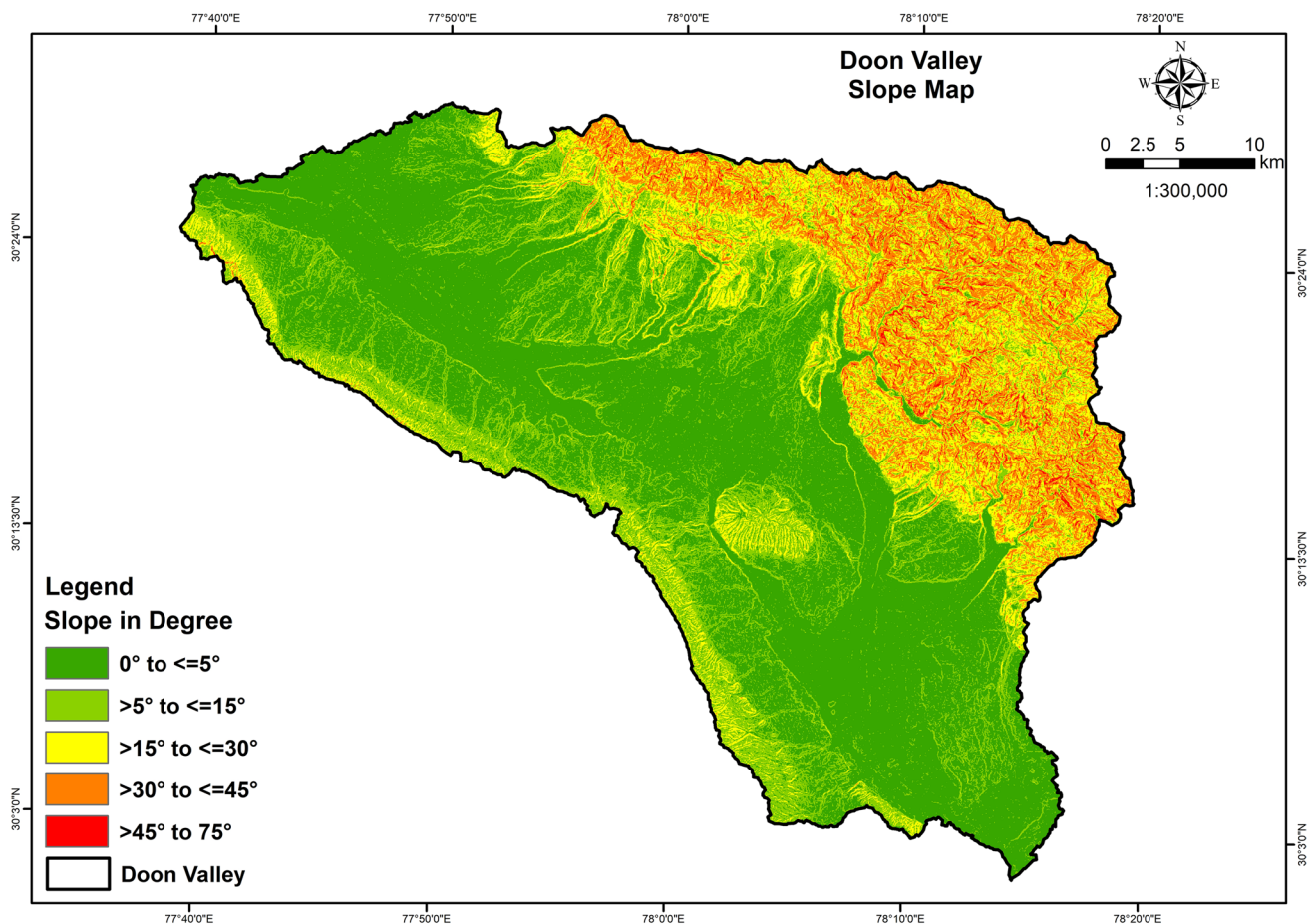
Fig. 3 Slope map

Table 2 Slope

Sr. No	Slope classes	Area in km^2	Area in %
1	0° to ≤ 5°	870.85	50.01
2	> 5° to ≤ 15°	369.46	21.21
3	> 15° to ≤ 30°	292.11	16.77
4	> 30° to ≤ 45°	188.85	10.84
5	> 45° to 75°	20.37	1.17
Total area		1741.64	100

4.3 Drainage density

The total length of streams per unit area is what is referred to as the drainage density. The subdivision of the landscape and the catchment area's potential for runoff are measured by drainage density. A greater degree of land subdivision indicates a greater probability of slope failure [34]. As indicated in Fig. 5, the drainage density is classified into five classes: (≤ 3 km/km^2) is very low, having 11.94% of the total area, (> 3 km/km^2 to ≤ 5 km/km^2) is low having 35.68% of the total area, (> 5 km/km^2 to ≤ 7 km/km^2) is moderate having 37.79% of the total area, (> 7 km/km^2 to ≤ 9 km/km^2) is high having 11.35% of the total area and (> 9 km/km^2 to 10.60 km/km^2) is very high having 3.24% of the total area. The majority portion of the total area has a medium to low drainage density (Table 4). The red color on the map denotes the area with the highest drainage density. The subdivision of the landscape and the catchment area's potential for runoff are measured by drainage density. A greater degree of land subdivision indicates a greater probability of slope failure.
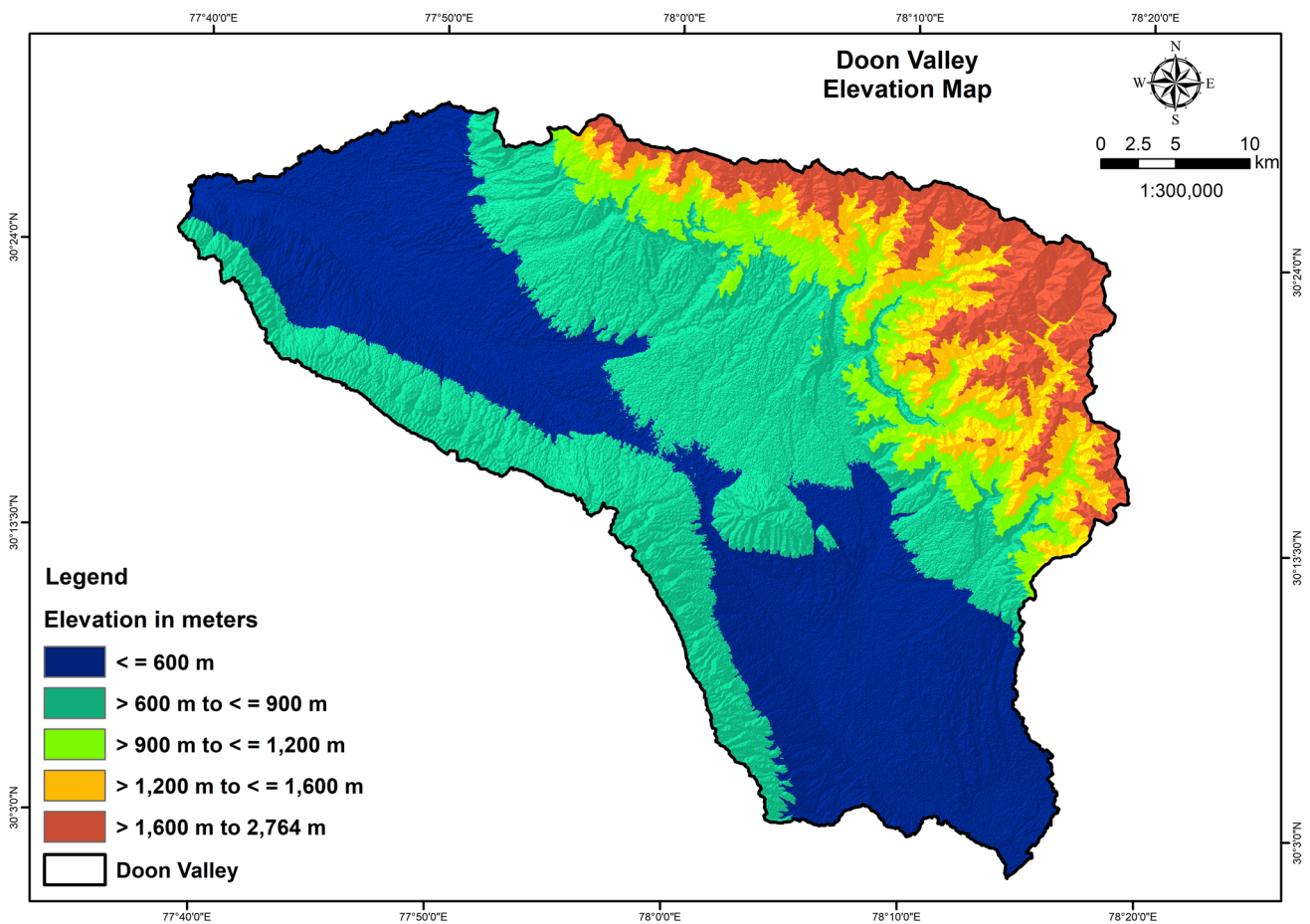
Fig. 4 Elevation map

Table 3 Elevation

Sr. No	Elevation classes	Area in km^2	Area in %
1	≤ 600 m	678.74	38.97
2	> 600 m to ≤ 900 m	617.73	35.47
3	> 900 m to ≤ 1200 m	131.47	7.54
4	> 1200 m to ≤ 1600 m	146.22	8.4
5	> 1600 m to 2764 m	167.48	9.62
Total area		1741.64	100

4.4 Geology

Geology formation becomes important in the study of landslides. The 11 classes of geology formation were shown in Fig. 6: Alluvium, Blaini/Infrakrol, Chandpur, Damta, Krol Sandstone + Krol A, Low Grade, Lower Tal, Middle Shiwalik, Nagthat, Upper Shiwalik, and Upper Tal. The Alluvium Formation has 62.62% of the total area, followed by the Upper Shiwalik Formation (Table 5). The Krol, Nagthat, Blaini, and Chandpur formations are more prone to landslides as compared with the Shiwalik formations [35, 36].
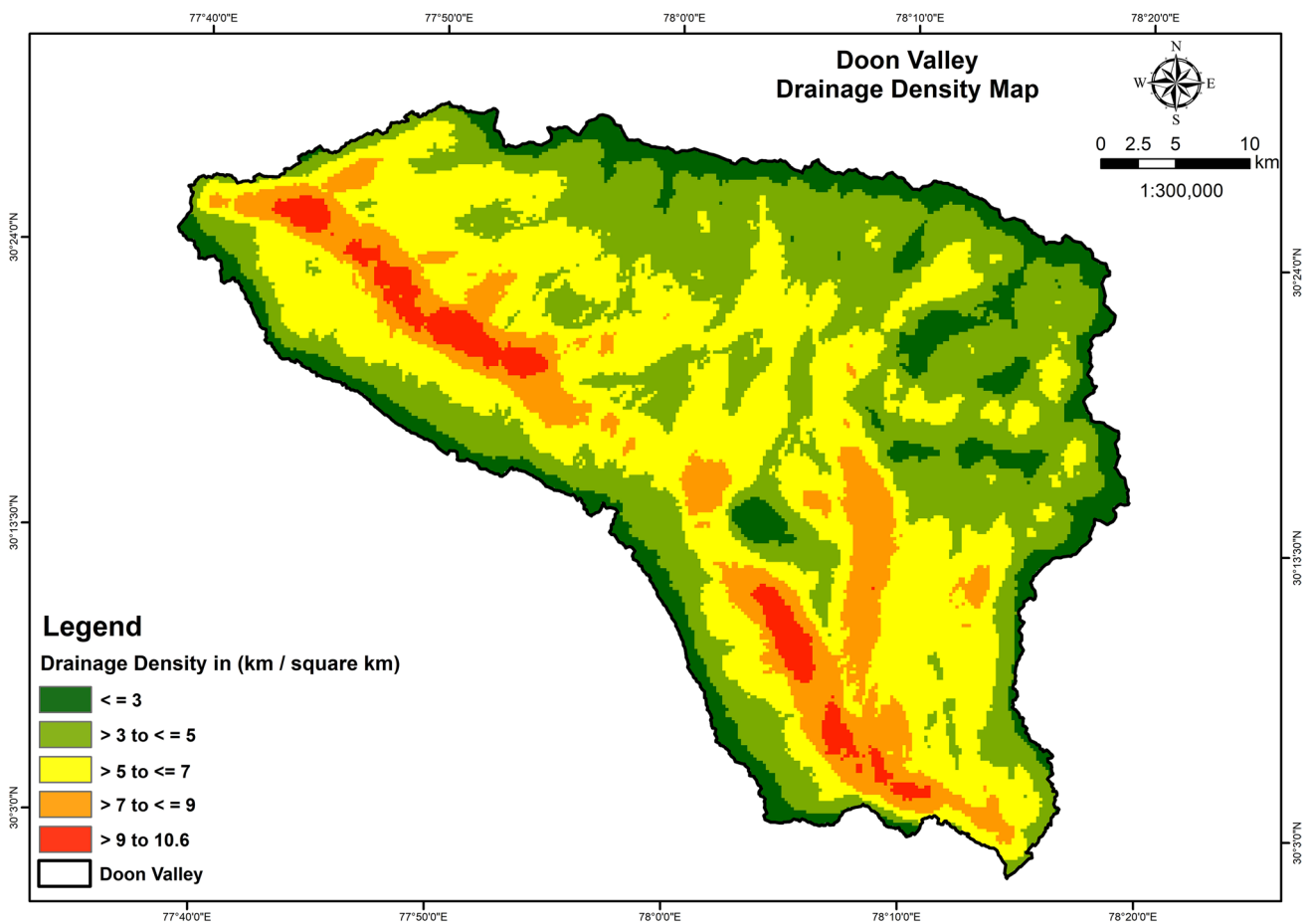
Fig. 5 Drainage density map

Table 4 Drainage density

Sr. No	Drainage density (km/km^2)	Area in km^2	Area in %
1	≤ 3	207.87	11.94
2	> 3 to ≤ 5	621.42	35.68
3	> 5 to ≤ 7	658.18	37.79
4	> 7 to ≤ 9	197.69	11.35
5	> 9 to 10.60	56.48	3.24
Total		1741.64	100

4.5 Soil type

Soil Type is an important parameter for LHZ Mapping. The Soil Type was classified into five Classes (Fig. 7): Sandy-Skeletal, Loamy-Skeletal, Coarse-Loamy, Fine-Loamy, Clayey, and Waterbodies [37]. The Majority of the area has Loamy-Skeletal soil types followed by Coarse-Loamy (Table 6). Loamy-Skeletal and Clayey soil types are more susceptible to landslides due to the presence of colluvium as a parent material.
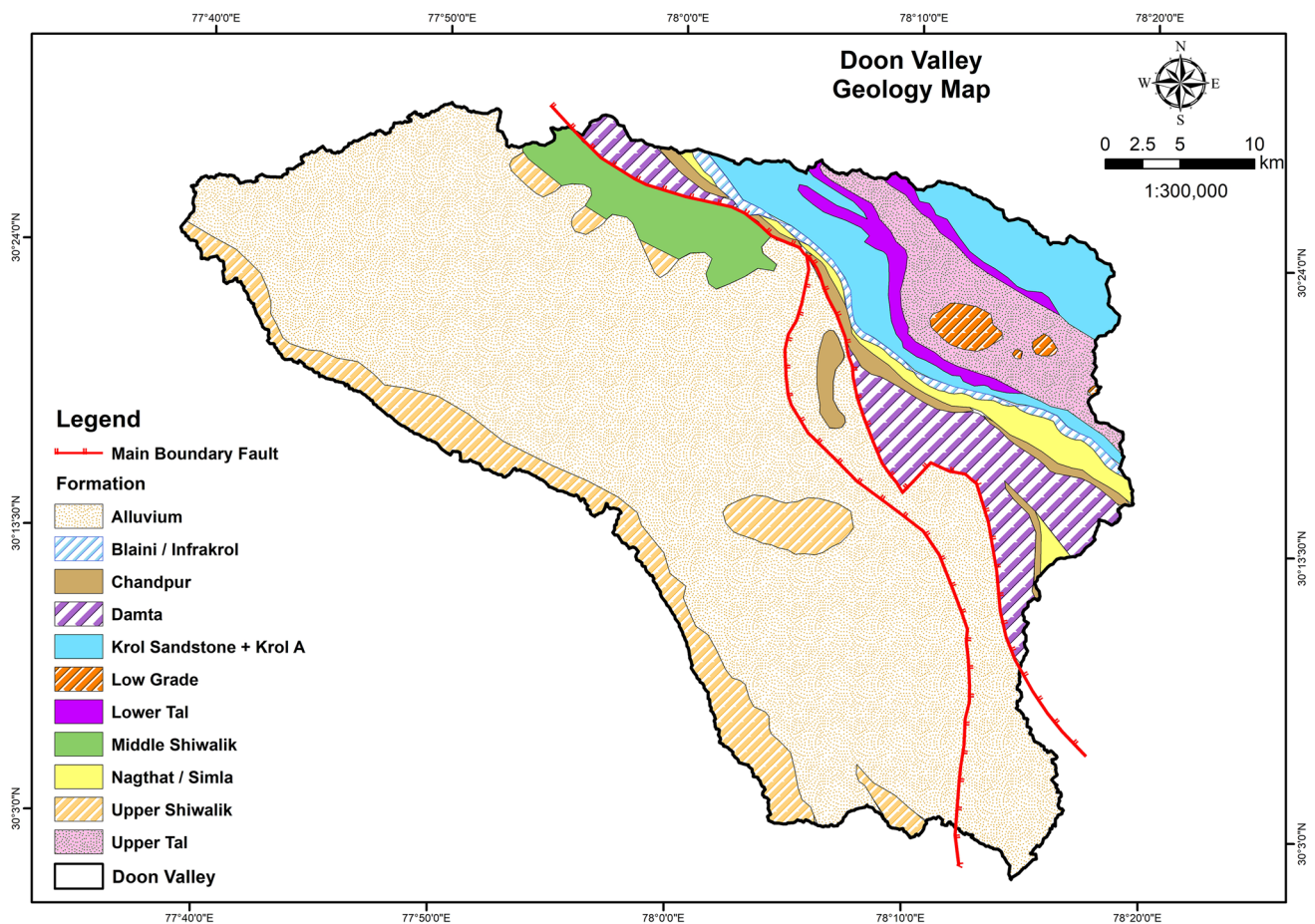
Fig. 6 Geology map

Table 5 Geology formation

Sr. No	Formations	Area in km²	Area in %
1	Alluvium	1090.65	62.62
2	Blaini/Infrakrol	16.55	0.95
3	Chandpur	32.57	1.87
4	Damta	117.95	6.77
5	Krol Sandstone + Krol A	110.74	6.36
6	Low Grade	13.09	0.75
7	Lower Tal	30.63	1.77
8	Middle Shiwalik	58.92	3.38
9	Nagthat	31.84	1.83
10	Upper Shiwalik	148.4	8.52
11	Upper Tal	90.3	5.18
Total Area		1741.64	100

4.6 Vegetation

Vegetation Types play an important role in landslide susceptibility mapping. The vegetation type map was created using NDVI, or Normalized Differential Vegetation Index. The formula for calculating the NDVI is (NIR-Red)/(NIR + Red) where (NIR) is (Band 8) and (Red) is (Band 4) of Sentinel-2B. The three classes of vegetation types are shown in Fig. 8:
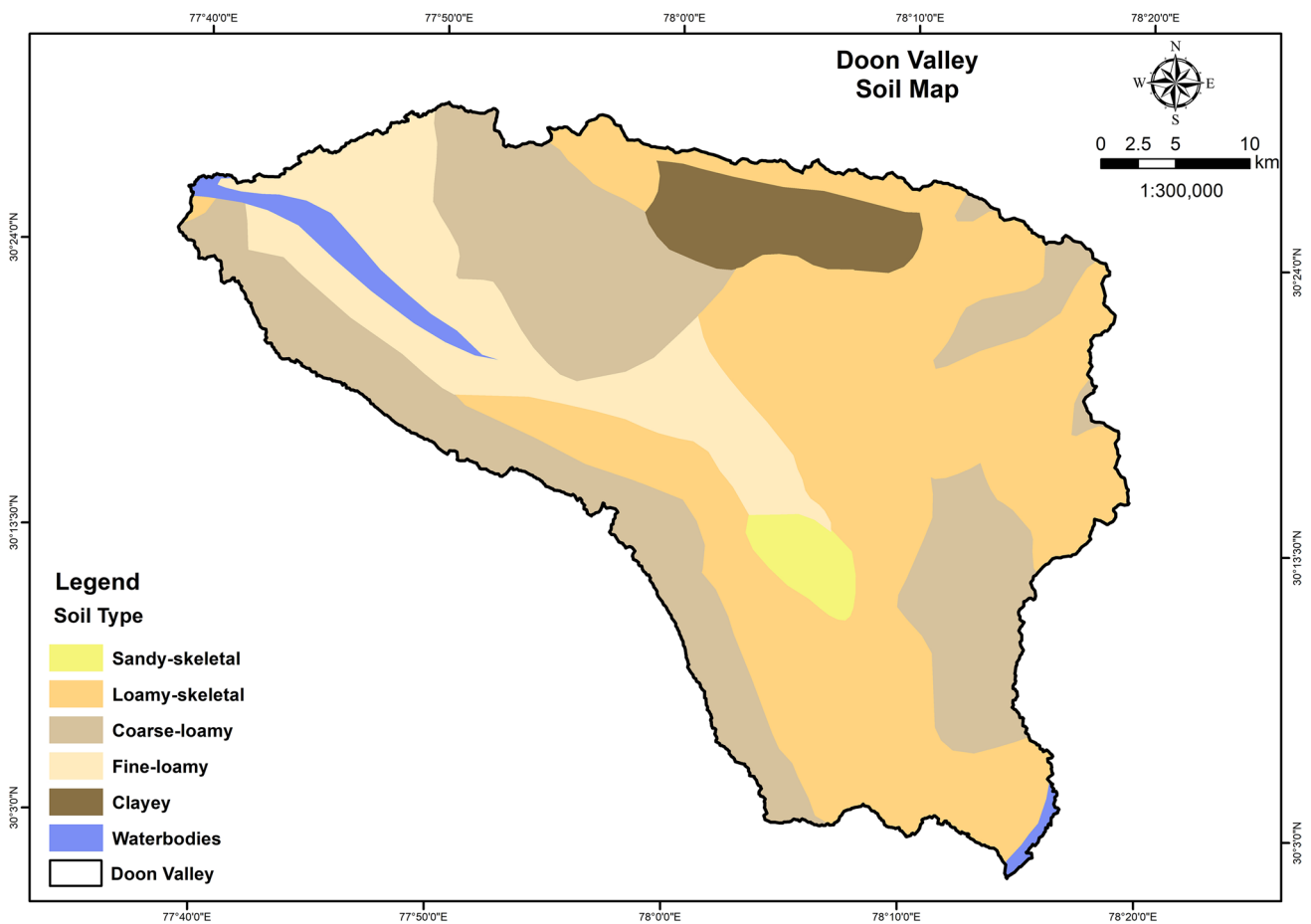
Fig. 7 Soil map

Table 6 Soil types

Sr. No	Soil types	Area in km^2	Area in %
1	Sandy-Skeletal	32.53	1.87
2	Loamy-Skeletal	768.82	44.14
3	Coarse-Loamy	560.42	32.18
4	Fine-Loamy	252.44	14.49
5	Clayey	90.74	5.21
6	Waterbodies	36.69	2.11
Total Area		1741.64	100

Dense Vegetation, Sparse Vegetation, and Barren Land. According to the vegetation types, Dense vegetation trees/plants with deep roots have contributed to an improvement in slope stability [38]. The Barren Land class, 23.1% of the total area, is more susceptible to landslide (Table 7).

4.7 Land use land cover LULC

Another essential factor for determining the Landslide Hazard Zone of any region is the LULC classification. It illustrates how anthropogenic activities, particularly urbanization, and agriculture, utilized land resources [39]. Due to climate change and land use practices, water resources are constantly under intense pressure. The LULC can be used to extrapolate the complicated physical processes occurring on the earth's surface [40, 41]. Sentinel-2B imagery was used to create the LULC map. For LULC classification, the ERDAS Imagine software uses the supervised classification
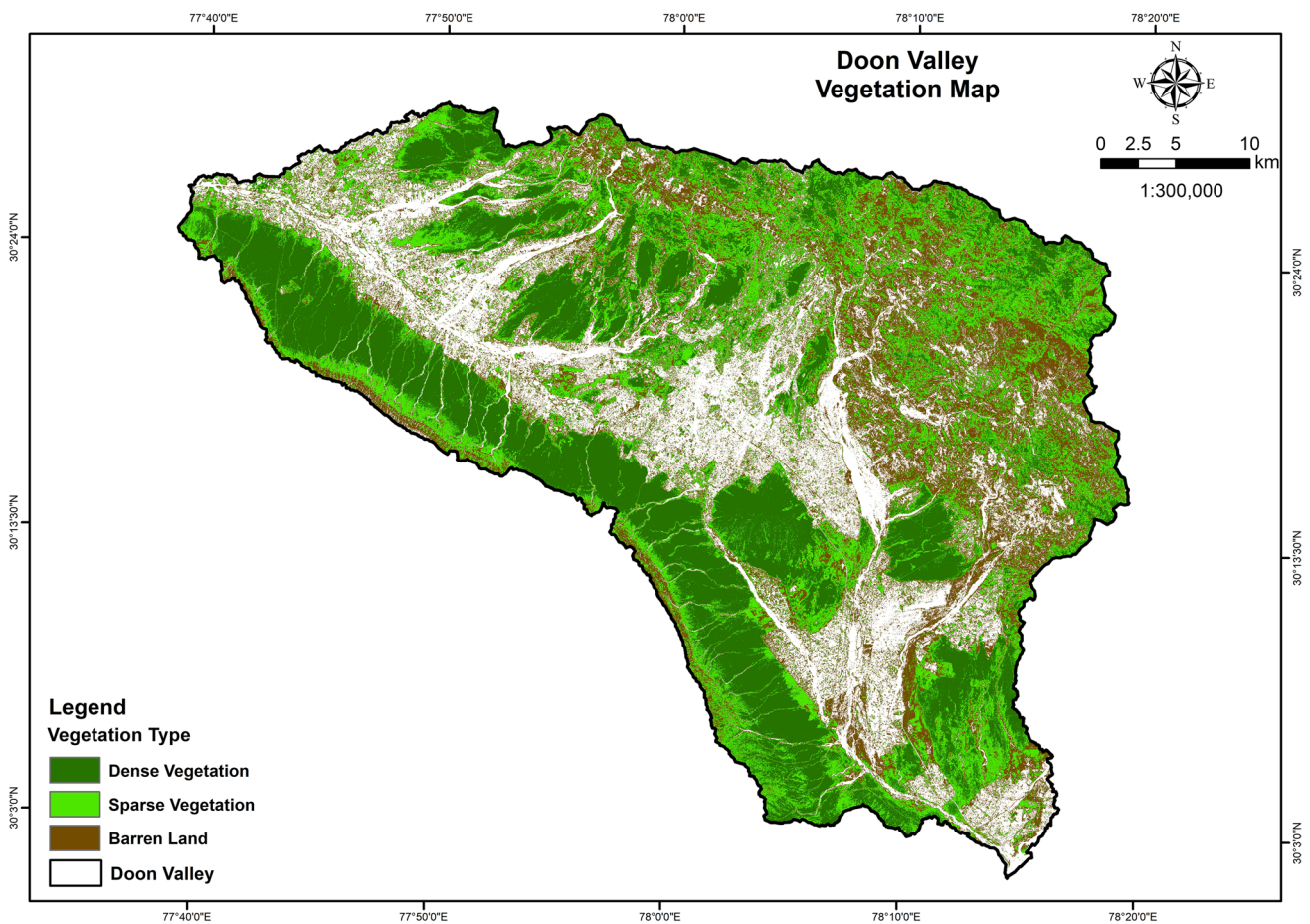
Discover

Fig. 8 Vegetation types map

Table 7 Vegetation types

Sr. No	Vegetation types	Area in km^2	Area in %
1	Dense vegetation	495.06	28.43
2	Sparse Vegetation	410.06	23.54
3	Barren land	402.31	23.1
4	No vegetation	434.21	24.93
Total area		1741.64	100

method. There are 6 LULC classes, as illustrated in Fig. 9: built-up, Agriculture Land, Forest Area, Wasteland, Dry Riverbed, and Waterbodies. The map's conclusion shows that Forest Area covered more than half of the total area (69.21%), followed by Agricultural Land (11.49%) (Table 8). Another dominant class is the Built-up, which takes up 9.09% of the space. The center of the valley has an anthropogenic load that directly affects the biodiversity and health of the rivers like Rispana, Bindal, Suswa, and Asan. The Wasteland covers the area 7.27% area of the Doon Valley. The two categories taking up the least amount of area are Waterbodies and Dry Riverbeds. Increasing tourist pressure in hilly region, changing climate are potentials risks due to landslide [42]. Tourism activities can lead to deforestation, soil erosion, and infrastructure stress, while climate change contributes to more intense and frequent rainfall. Together, these factors destabilize slopes, increasing the likelihood of landslides. Runoff from agricultural activities can significantly increase the risk of erosion and landslides in riverine areas. Excess water from irrigation and rainfall reduce soil stability. This, combined with the removal of vegetation for agriculture, can accelerate soil erosion and trigger landslides along riverbanks [43].
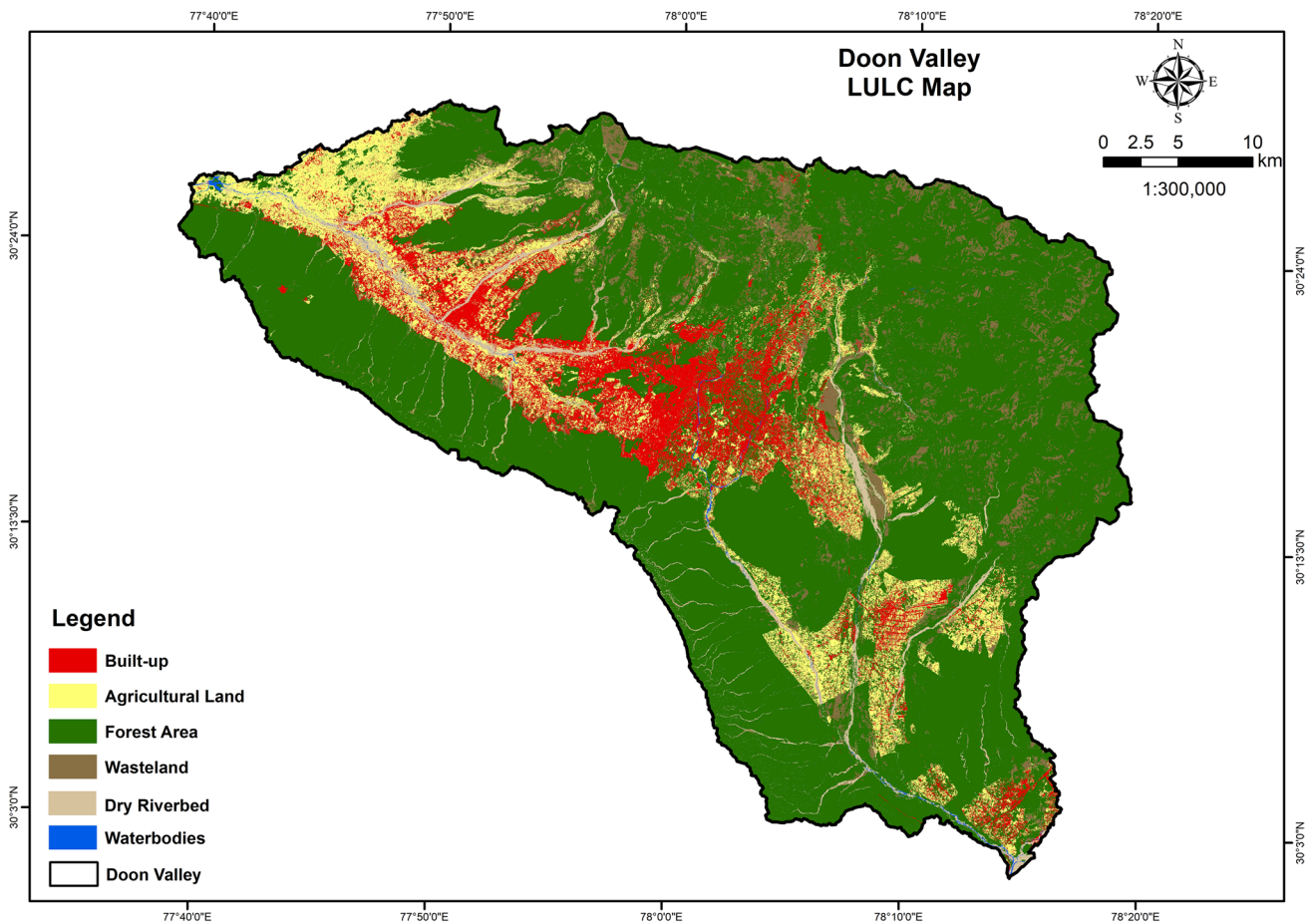
Fig. 9 LULC map

Table 8 LULC classes

Sr. No	LULC classes	Area in km^2	Area in %
1	Built-up	158.26	9.09
2	Agricultural land	200.17	11.49
3	Forest area	1205.4	69.21
4	Wasteland	126.7	7.27
5	Dry riverbed	47.35	2.72
6	Waterbodies	3.76	0.22
Total area		1741.64	100

4.8 Aspect

The Aspect displays the slope's direction. The Aspect at (0°–22.5°) is north, at (22.5°–67.5°) Northeast, and so on. For this study, the direction of the slope is on two sides, one west-facing and another southwest- south facing as shown in Fig. 10 & Table 9. In comparison to the east-facing slope, the west and south-facing slope has more vegetation cover and more moisture.

4.9 Landslide hazard zonation (LHZ) mapping

The LHZ mapping is a crucial tool for mitigating the risk associated with landslides. Different spatial data sources, including topography, geology, LULC, vegetation, and soil characteristics, must be integrated during the process [44]. The LHZ
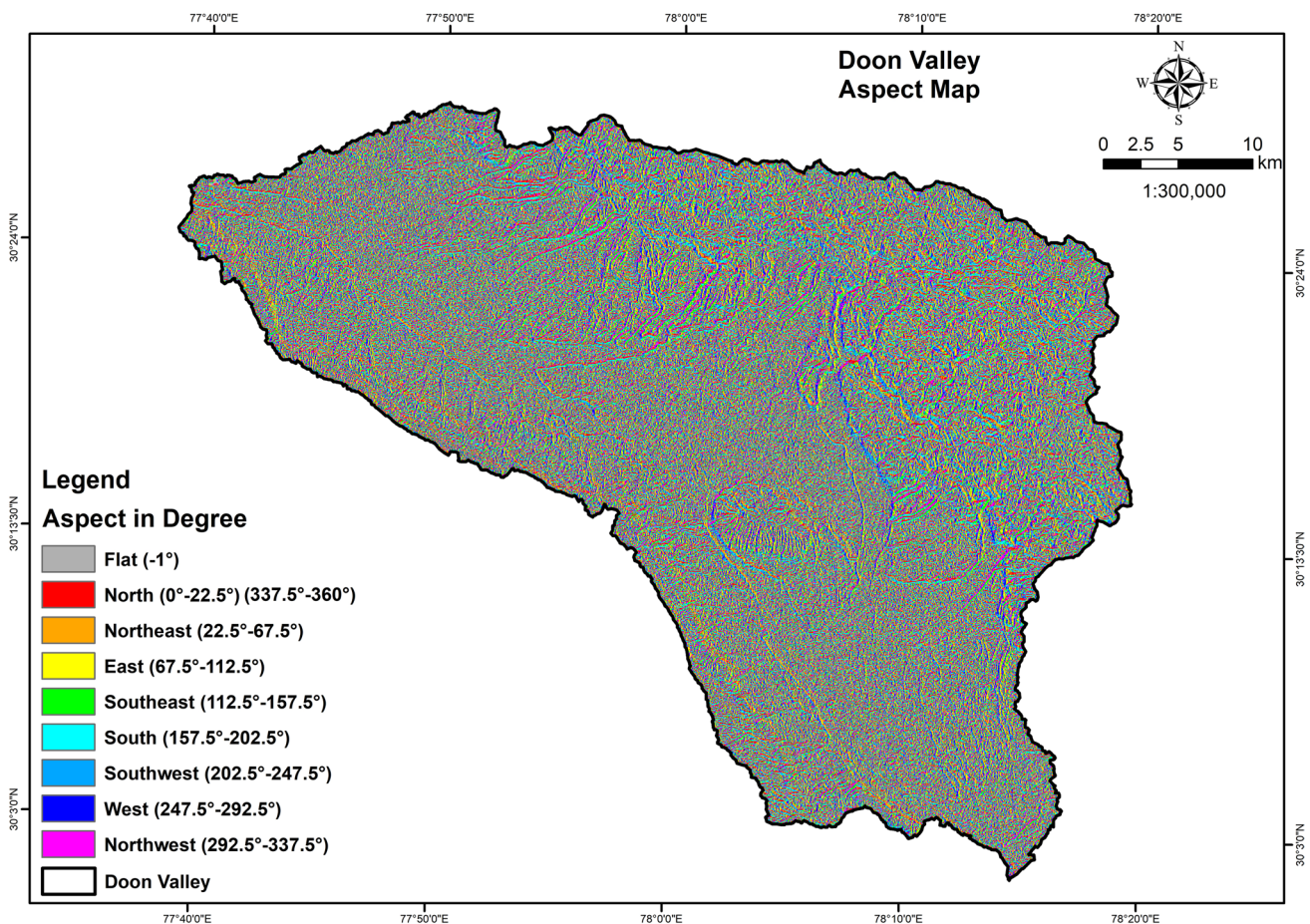
Fig. 10 Aspect map

Table 9 Aspect classes

Sr. No	Aspect classes	Area in km²	Area in %
1	Flat (− 1°)	0.1	0.006
2	North (0°–22.5°) (337.5°–360°)	223.33	12.823
3	Northeast (22.5°–67.5°)	203.88	11.706
4	East (67.5°–112.5°)	221.5	12.718
5	Southeast (112.5°–157.5°)	219.73	12.616
6	South (157.5°–202.5°)	225.77	12.963
7	Southwest (202.5°–247.5°)	205	11.771
8	West (247.5°–292.5°)	223.11	12.81
9	Northwest (292.5°–337.5°)	219.22	12.587
	Total area	1741.64	100

map gives a thorough picture of how the landslide risk is distributed spatially within an area and can be used to guide decision-making for disaster management, land use planning, and infrastructure development. The LHZ map was created using the Weighted Overlay method in ArcGIS Software. Weighted Overlay is a multi-criteria analysis between several raster layers. For this study, the eight raster layers were used and given the rank (R_i) from 8 to 1, where 8 means highest and 1 means lowest. Each raster layer is further divided into different classes and given the weightage (W_i) from 1 (lowest) to 8 (highest). Also, the percent influence (%) of each raster layer from the overall 100% is mentioned in Table 10.

As depicted in Fig. 11, there are five classes that make up the Landslide Hazard Zones: very high hazard zone, high hazard zone, medium hazard zone, low hazard zone, and very low hazard zone. According to Table 11, 16.64% of the

Table 10 Rank, influence and weightage of factors for landslide

Factor	Classes	Rank (R_f)	Influence (%)	Weight-age (W_f)	Remarks
LULC	Waterbodies	8	20%	1	Improper land use such as wasteland, Dry River bed and Built-up in hilly regions have a higher susceptibility to landslides
	Forest Area			2	
	Agricultural Land			3	
	Built-up			5	
	Dry Riverbed			7	
	Wasteland			8	
Slope	0° to ≤5°	7	15%	1	Since, there is presence of Debris covering the slope surface, steeper slopes above 45° are more susceptible to landslides than slopes less than 15°
	>5° to ≤15°			2	
	>15° to ≤30°			5	
	>30° to ≤45°			7	
	>45° to 75°			8	
Geology	Alluvium	6	15%	1	Due to the existence of f debris, faults, trust, etc., Krol, Damta and Chandpur formations are extremely sensitive
	Upper Shiwalik			2	
	Middle Shiwalik			6	
	Nagthat			6	
	Upper Tal			7	
	Lower Tal			7	
	Low grade			7	
	Blaini/Infrakrol			7	
	Chandpur			8	
	Damta			8	
	Krol Sandstone + Krol A			8	
Soil Type	Waterbodies	5	15%	1	Due to colluvium parent material, soil types that are Clayey and Loamy-Skeletal are more prone to landslides
	Sandy-Skeletal			2	
	Fine-Loamy			4	
	Coarse-Loamy			6	
	Loamy-Skeletal			7	
	Clayey			8	
Elevation	≤600 m	4	10%	1	Due to the abundance of debris, fragments, etc., elevation ranges greater than 1200 m are particularly vulnerable to landslides
	>600 m to ≤900 m			2	
	>900 m to ≤1200 m			5	
	>1200 m to ≤1600 m			7	
	>1600 m to 2764 m			8	

Table 10 (continued)

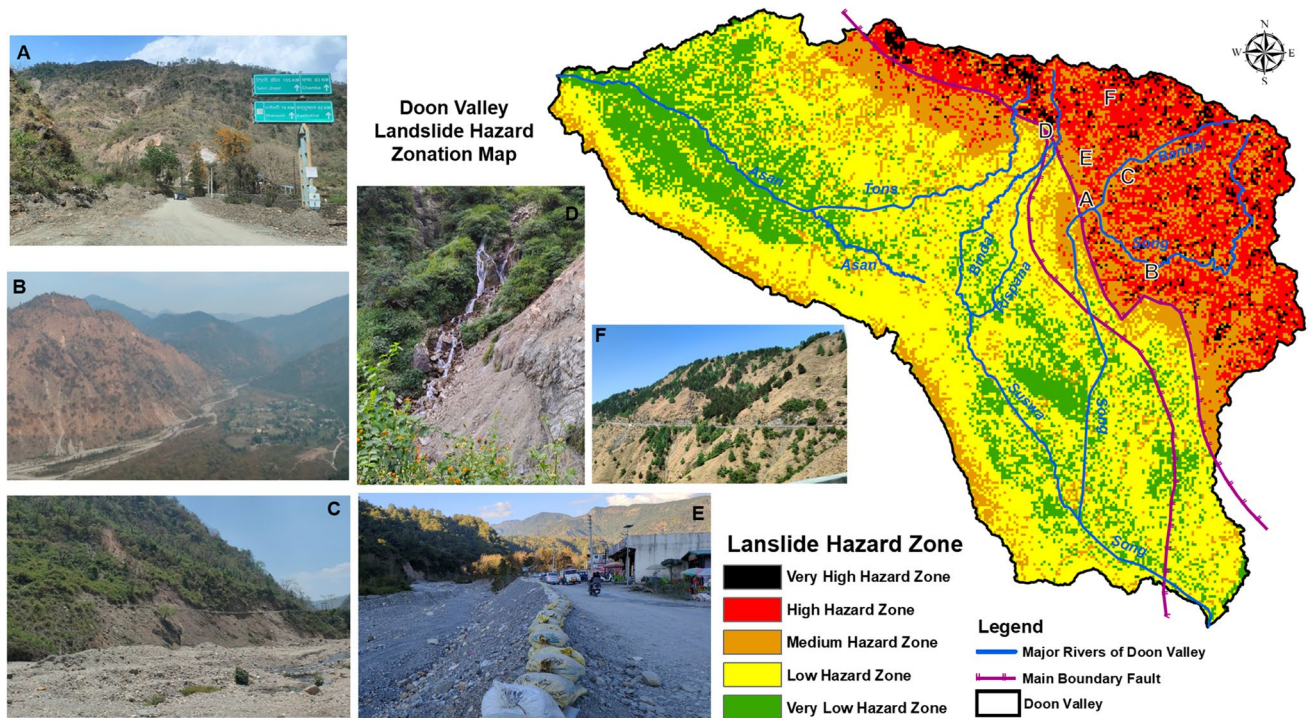| Factor	Classes	Rank (R_i)	Influence (%)	Weight-age (W_i)	Remarks
Drainage Density	>9 to 10.60	3	10%	1	Less drainage density increases the probability of infiltration, which increases pore pressure and causes landslides
	>7 to ≤9			2	
	>5 to ≤7			5	
	>3 to ≤5			7	
	≤3			8	
Vegetation	Dense vegetation	2	10%	1	The possibility of landslides increases on Barren Land
	Sparse vegetation			5	
	Barren Land			8	
Aspect	Flat (− 1°)	1	5%	1	Due to the direction of the wind, direct sunlight, and rainfall, the North, Northeast, and Northwest directions of slope are more susceptible to landslides
	South (157.5°–202.5°)			1	
	Southwest (202.5°–247.5°)			2	
	Southeast (112.5°–157.5°)			3	
	East (67.5°–112.5°)			4	
	West (247.5°–292.5°)			5	
	Northwest (292.5°–337.5°)			6	
	Northeast (22.5°–67.5°)			7	
	North (0°–22.5°) (337.5°–360°)			8	

Fig. 11 Landslide hazard zonation map with photographs of landslides in Doon Valley

Table 11 LHZ table

Sr. No	Landslide hazard zones	Area in km^2	Area in %
1	Very high hazard zone	45.48	2.61
2	High hazard zone	244.39	14.03
3	Medium hazard zone	370.6	21.28
4	Low hazard zone	769.61	44.19
5	Very low hazard zone	311.56	17.89
	Total area	1741.64	100

total area is located near and above the Main Boundary Thrust/Fault (MBT), which is prone to landslides, and is classified as being in the high to very high hard zone. The upper stretches of the Doon Valley rivers are more significant to landslides than the lower stretches because steep slope, high elevation and presence of Krol, Nagthat, Blaini, and Chandpur geological formations. River ecosystems can be significantly impacted by landslides, which can change the water's physical and chemical properties as well as the river's biodiversity. Landslides can result in significant amounts of sediment and debris entering rivers, which lowers water quality and raises turbidity [45]. The loss of crucial fish breeding habitat and the deposition of fine sediment in river beds are both potential effects of the increased sediment load [46]. Recent event of cloud burst on 19th and 20th August, 2022 have triggered the landslide in many regions of Doon Valley and washes away the banks of river Bandal and Song [47]. Increasing population and uncontrolled tourism in the valley is contributing to the occurrence of landslides by placing additional pressure on vulnerable landscapes and altering natural terrain [48]. Not limited to this, landslides also cause changing in land uses of a particular area. The removal of vegetation cover due to landslides may cause more soil erosion, which in turn degrades the soil's quality and limits its capacity to support plant development [49]. In general, landslides can have a major impact on an area's LULC pattern, leading to a loss of vegetation cover, an increase in rocky areas and barren land, as well as a decrease in agricultural output. These effects may have long-term consequences for an area's environment and biodiversity, emphasizing the necessity for efficient landslide risk management and mitigation measures.

5 Conclusion

This study demonstrates a clear link between the factors: LULC, Slope, Geology, Soil Type, Elevation, Drainage Density, Vegetation, and Aspect, all are significant for the LHZ mapping. In-depth knowledge of the numerous landslide-causing factors and identification of the high-risk areas can be achieved through the use of advanced remote sensing and GIS techniques. The approach for the LHZ mapping includes the creation of thematic data layers, the incorporation of spatial data, and the validation of outcomes. The findings of this study clearly demonstrate that the area near and above the Main Boundary Thrust/Fault (MBT) is more susceptible to landslide. Also, the upper stretches of the Doon Valley rivers are much more vulnerable to landslides for habitat and biodiversity loss than the lower stretches. Anthropogenic activities such as construction of new houses/buildings and development of new roads/highways near the steep slope and very steep slope regions of the Doon Valley should be managed or planned sustainably. Additionally, understanding geological formations with changing land uses is vital for determining the region's susceptibility to landslides.

Overall, the LHZ mapping is a crucial part of risk assessment and management plans. It offers a reliable tool for decision-makers to comprehend possible dangerous locations and put in place the necessary safeguards to reduce the effects of landslides. Further research in this area is necessary to improve the accuracy of landslide hazard zonation maps and develop better mitigation strategies. For effective future use of the LHZ mapping, consider the following key recommendations: integrate multi-temporal satellite imagery to analyze land use and vegetation changes over time, enhancing trend identification and prediction. Apply machine learning algorithms for advanced pattern recognition and predictive modeling. Combine geological, hydrological, meteorological, and land use data for a comprehensive landslide risk model. Engage local communities in data collection and validation, and conduct regular field surveys to ensure map accuracy.

Data availability Data is provided within the manuscript files.

Declarations

Competing interests The authors declare no competing interests.

References

1. Aristizábal E, Sánchez O. Spatial and temporal patterns and the socioeconomic impacts of landslides in the tropical and mountainous Colombian Andes. Disasters. 2020;44(3):596–618.
2. Tiwari PC, Tiwari A, Joshi B. Urban growth in Himalaya: understanding the process and options for sustainable development. J Urban Reg Stud Contemp India. 2018;4(2):15–27.
3. Sujatha ER, Rajamanickam GV. Landslide hazard and risk mapping using the weighted linear combination model applied to the Tevankarai Stream Watershed, Kodaikkanal, India. Human Ecol Risk Assess. 2015;21(6):1445–61.
4. Geological Survey of India. Landslide hazard; 2023. https://www.gsi.gov.in/webcenter/portal/OCBIS/pages_pageGeoInfo/pageLANDSLIDEHAZRD
5. Allen SK, Rastner P, Arora M, Huggel C, Stoffel M. Lake outburst and debris flow disaster at Kedarnath, June 2013: hydrometeorological triggering and topographic predisposition. Landslides. 2016;13:1479–91. https://doi.org/10.1007/s10346-015-0584-3.

6. Sur U, Singh P, Rai PK, Thakur JK. Landslide probability mapping by considering fuzzy numerical risk factor (FNRF) and landscape change for road corridor of Uttarakhand, India. Environ Dev Sustain. 2021;23:13526–54. https://doi.org/10.1007/s10668-021-01226-1.

7. Mani A, Bansal D, Kumari M, Kumar D. Land use land cover changes and climate change impact on the water resources: a study of Uttarakhand State. In: River conservation and water resource management. Springer Nature Singapore: Singapore; 2023. p. 1–16.

8. Prakash S. Historical records of socio-economically significant landslides in India. J South Asia Disaster Stud. 2011;4(2):177–204.

9. Kumar A, Kumar A, Goyal RK. Landslide hazard zonation using geospatial techniques: a review. Nat Hazards. 2018;91(2):545–70.

10. Nagarajan R, Mukherjee A, Roy A, Khire MV. Temporal remote sensing data and GIS application in landslide hazard zonation of part of Western Ghat, India. Int J Remote Sens. 1998;19(4):573–85.

11. Saha AK, Gupta RP, Arora MK. GIS-based landslide hazard zonation in the Bhagirathi (Ganga) Valley, Himalayas. Int J Remote Sens. 2002;23(2):357–69.

12. Pandey A, Dabral PP, Chowdary VM, Yadav NK. Landslide hazard zonation using remote sensing and GIS: a case study of Dikrong river basin, Arunachal Pradesh, India. Environ Geol. 2008;54:1517–29.

13. Kumar KV, Nair RR, Lakhera RC. Digital image enhancement for delineating active landslide areas. Asia-Pac Remote Sens J. 1993;6(1):63–6.

14. Sakellariou MG, Ferentinou MD. GIS-based estimation of slope stability. Nat Hazard Rev. 2001;2(1):12–21.

15. Yamaguchi Y, Tanaka S, Odajima T, Kamai T, Tsuchida S. Detection of a landslide movement as geometric misregistration in image matching of SPOT HRV data of two different dates. Int J Remote Sens. 2003;24(18):3523–34.

16. Pieraccini M, Casagli N, Luzi G, Tarchi D, Mecatti D, Noferini L, Atzeni C. Landslide monitoring by ground-based radar interferometry: a field test in Valdarno (Italy). Int J Remote Sens. 2003;24(6):1385–91.

17. Casson B, Delacourt C, Baratoux D, Allemand P. Seventeen years of the "'La Clapie`re'" landslide evolution analysed from ortho-rectified aerial photographs. Eng Geol. 2003;68:123–39.

18. Glassey P, Barrell D, Forsyth J, Macleod R. The geology of Dunedin, New Zealand, and the management of geological hazards. Quatern Int. 2003;103:23–40.

19. Lee S, Ryu JH, Won JS, Park HJ. Determination and application of the weights for landslide susceptibility mapping using an artificial neural network. Eng Geol. 2003;71(3–4):289–302.

20. Velayudham J, Kannaujiya S, Sarkar T, Ray PKC, Taloor AK, Bisht MPS, Chawla S, Pal SK. Comprehensive study on evaluation of Kaliasaur Landslide attributes in Garhwal Himalaya by the execution of geospatial, geotechnical and geophysical methods. Quat Sci Adv. 2021;3: 100025. https://doi.org/10.1016/j.qsa.2021.100025.

21. Taloor AK, Kothyari GC, Goswami A, Mishra A. Geospatial technology applications in Quaternary Science. Quat Sci Adv. 2022;7: 100059. https://doi.org/10.1016/j.qsa.2022.100059.

22. Taloor AK, Dumka RK, Kothyari GC, Srivastava P, Khare N. Active tectonics and surface processes using geospatial technology. J Appl Geophys. 2023;215: 105140. https://doi.org/10.1016/j.jappgeo.2023.105140.

23. Wang F, Qin C, Zhang J, Chen X, Feng W. GIS-based landslide susceptibility mapping using analytic hierarchy process and logistic regression model: a case study in Yihuang County, China. Arab J Geosci. 2018;11(14):356.

24. Huang X, Jiang Y, Chen Y, Chen Z, Chen Y. A new method for landslide hazard zoning based on remote sensing and GIS: a case study in Guangxi Province, China. CATENA. 2020;189: 104493.

25. Taloor AK, Abraham A, Parsad G. Landslide susceptibility modelling in the Doda Kishtwar ramban (DKR) region of Jammu and Kashmir using remote sensing and geographic information system. Quat Sci Adv. 2024;14: 100189. https://doi.org/10.1016/j.qsa.2024.100189.

26. Shit PK, Bhunia GS, Maiti R. Potential landslide susceptibility mapping using weighted overlay model (WOM). Model Earth Syst Environ. 2016. https://doi.org/10.1007/s40808-016-0078-x.

27. Mani A, Kumari M, Badola R. Morphometric analysis of Suswa River Basin using geospatial techniques. Eng Proc. 2022;27(1):65.

28. Jasrotia AS, Kumar A, Aasim M. Morphometric analysis and hydrogeomorphology for delineating groundwater potential zones of Western Doon Valley, Uttarakhand, India. Int J Geomatics Geosci. 2011;2(4):1078–96.

29. Mani A, Kumari M, Badola R. A GIS-based assessment of Asian River Basin for watershed management. In Proceedings of 42nd INCA international congress on digital cartography to harness blue economy. Dehradun: INCA; 2023.

30. Jasrotia AS, Taloor AK, Andotra U, Bhagat BD. Geoinformatics based groundwater quality assessment for domestic and irrigation uses of the Western Doon valley, Uttarakhand, India. Groundw Sustain Dev. 2018;6:200–12.

31. Mani A, Kumar D. Morphometric analysis of Manali Watershed of Beas River Basin for Watershed Management. VayuMandal. 2020;46:21–9.

32. Anbalagan R. Landslide hazard evaluation and zonation mapping in mountainous terrain. Eng Geol. 1992;32:269–77.

33. Mani A, Kumari M, Badola R. Evaluating urban topography and land use changes for urban river management using geospatial techniques. Eng Proc. 2023;58(1):12.

34. Versain LD, Banshtu RS, Pandey DD. Comparative evaluation of GIS based landslide hazard zonation maps using different approaches. J Geol Soc India. 2019;93(6):684–92.

35. Rupke J, Sharma RP. Preliminary geological map of Western Kumaon Himalayas. In: Stratigraphic and Structural evolution of Kumaon Lesser Himalayas, vol. 11. Sed Geology; 1974. p. 81–265.

36. Pachauri AK, Pant M. Landslide hazard mapping based on geological attributes. Eng Geol. 1992;32:81–100.

37. ICAR-NBSS & LUP, Bhoomi Geoportal. http://14.139.123.73:9090/web/bhoomi2.0.php

38. Greenway DR. Vegetation and slope stability. In: Anderson MG, Richards KS, editors. slope stability. New York: Wiley; 1987. p. 187–230.

39. YanYun NIAN, Xin LI, Jian ZHOU, XiaoLi HU. Impact of land use change on water resource allocation in the middle reaches of the Heihe River Basin in Northwestern China. J Arid Land. 2014;6(3):273–86.

40. Dai F, Lee C. Landslide characteristics and slope instability modeling using GIS, Lantau Island, Hong Kong. Geomorphology. 2002;42(3–4):213–28.

41. Bera A, Mukhopadhyay BP, Das D. Landslide hazard zonation mapping using multi-criteria analysis with the help of GIS techniques: a case study from Eastern Himalayas, Namchi, South Sikkim. Nat Hazards. 2019;96:935–59.

42. Mani A, Kumar D, Kumar D (2021) Evaluating decadal change in green cover of Dehradun City. In: Geospatial technology and smart cities. p. 469–483. https://doi.org/10.1007/978-3-030-71945-6_26

43. Garcia-Chevesich P, Wei X, Ticona J, Martínez G, Zea J, García V, Alejo F, Zhang Y, Flamme H, Graber A, Santi P, McCray J, Gonzáles E, Krahenbuhl R. The impact of agricultural irrigation on landslide triggering: a review from Chinese, English, and Spanish Literature. Water. 2020. https://doi.org/10.3390/w13010010.

44. Pareta K, Pareta U. Integrated watershed modeling and characterization using GIS and remote sensing techniques. Indian J Eng. 2012;1(1):81–91.

45. Sullivan K. Long-term patterns of water quality in a managed watershed in Oregon: 1. Suspended sediment. J Am Water Resour Assoc. 1985;21(6):977–87.

46. Kemp P, Sear D, Collins A, Naden P, Jones I. The impacts of fine sediment on riverine fish. Hydrol Process. 2011;25(11):1800–21.

47. Sain K, Mehta M, Kumar V, Gupta V, Chauhan P. A climatic surprise-slope instability triggered by heavy rain in Maldevta Region, Dehradun, Uttarakhand, on 20 August, 2022. J Geol Soc India. 2023;99:317–20. https://doi.org/10.1007/s12594-023-2313-1.

48. Census of India. Dehradun District; 2011. https://www.census2011.co.in/census/district/578-dehradun.html

49. Zuazo VHD, Pleguezuelo CRR. Soil-erosion and runoff prevention by plant covers: a review. In: Lichtfouse E, Navarrete M, Debaeke P, Véronique S, Alberola C, editors. Sustainable agriculture. Springer; 2009. p. 785–811.